Labeit, S., Barlow, D. P., Gautel, M., Gibson, T., Holt, J., Hsieh, C. L., Francke, U., Leonard, K., Wardale, J., Whiting, A., & Trinick, J. (1990) *Nature 345*, 272–276.
Marion, D., & Bax, A. (1988) *J. Magn. Reson. 79*, 352–356.
Marion, D., Ikura, M., & Bax, A. (1989) *J. Magn. Reson. 84*, 425–430.
Mellor, J., Dobson, M. J., Roberts, N. A., Tuite, M. F., Emtage, J. S., White, S., Lowe, P. A., Patel, T., Kingsman, A. J., & Kingsman, S. M. (1983) *Gene 24*, 1–14.
Messerle, B. A., Wider, G., Otting, G., Weber, C., & Wüthrich, K. (1989) *J. Magn. Reson. 85*, 608–613.
Moos, M., Tacke, R., Scherer, H., Teplow, D., Früh, K., & Schachner, K. (1988) *Nature 334*, 701–703.
Norwood, T. J., Boyd, J., Heritage, J. E., Soffe, N., & Campbell, I. D. (1990) *J. Magn. Reson. 87*, 488–501.
Obara, M., Kang, M. S., & Yamada, K. M. (1988) *Cell 53*, 649–657.
Patthy, L. (1991) *Curr. Opin. Struct. Biol. 1*, 351–361.
Pierschbacher, M. D., & Ruoslahti, E. *Nature 309*, 30–33.
Plateau, P., & Gueron, M. (1982) *J. Am. Chem. Soc. 104*, 7310–7311.
Rance, M., Sorensen, O. W., Bodenhausen, G., Wagner, G., Ernst, R. R., & Wüthrich, K. (1983) *Biochem. Biophys. Res. Commun. 117*, 479–485.
Ruoslahti, E. (1988) *Annu. Rev. Biochem. 57*, 375–413.
Ryu, S. E., Kwong, P. D., Truneh, A., Porter, T. G., Arthos, J., Rosenberg, M., Dai, X., Xuong, N., Axel, R., Sweet, R. W., & Hendrickson, W. A. (1990) *Nature 348*, 419–425.
Williams, A. F., & Barclay, N. (1988) *Annu. Rev. Immunol. 6*, 381–405.
Wüthrich, K. (1986) *NMR of Proteins and Nucleic Acids*, Wiley-Interscience, New York.
Yamada, K. M., & Kennedy, D. W. (1984) *J. Cell Biol. 99*, 29–36.

$^{14,15}N$, ^{13}C, ^{57}Fe, and $^{1,2}H$ Q-Band ENDOR Study of Fe–S Proteins with Clusters That Have Endogenous Sulfur Ligands†

Andrew L. P. Houseman,‡ Byung-Ha Oh,§ Mary Claire Kennedy,∥ Chaoliang Fan,‡ Melanie M. Werst,‡ Helmut Beinert,∥ John L. Markley,§ and Brian M. Hoffman*,‡

Department of Chemistry, Northwestern University, 2145 Sheridan Road, Evanston, Illinois 60208-3113, Department of Biochemistry, College of Agriculture and Life Sciences, University of Wisconsin—Madison, 420 Henry Hall, Madison, Wisconsin 53706, and Department of Biochemistry and National Biomedical ESR Center, Medical College of Wisconsin, 8701 Watertown Plank Road, Milwaukee, Wisconsin 53226

Received August 23, 1991; Revised Manuscript Received November 8, 1991

ABSTRACT: The benefits of performing ENDOR experiments at higher microwave frequency are demonstrated in a Q-band (35 GHz) ENDOR investigation of a number of proteins with [*n*Fe–*m*S] clusters, $n = 2, 3, 4$. Each protein displays several resonances in the frequency range of 0–20 MHz. In all instances, features are seen near $\nu \approx 13$ and 8 MHz that can be assigned, respectively, to "distant ENDOR" from ^{13}C in natural-abundance (1.1%) and from ^{14}N (the $\Delta m_I = \pm 2$ transitions); the nuclei involved in this phenomenon are remote from and have negligible hyperfine couplings to the cluster. In addition, a number of proteins show local ^{13}C ENDOR signals with resolved hyperfine interactions; these are assigned to the β carbons of cysteines bound to the cluster [$A(^{13}C) \approx 1.0$ MHz]. Five proteins show resolved, local $\Delta m_I = \pm 2$ ENDOR signals from ^{14}N with an isotropic hyperfine coupling, $0.4 \lesssim A(^{14}N) \lesssim 1.0$, similar to those seen in ESEEM studies; these most likely are associated with N–H···S hydrogen bonds to the cluster. *Anabaena* ferredoxin further shows a signal corresponding to $A(^{14}N) \approx 4$ MHz. Quadrupole coupling constants are derived for both local and distant ^{14}N signals. The interpretation of the data is supported by studies on ^{15}N- and ^{13}C-enriched ferredoxin (Fd) from *Anabaena* 7120, where the ^{15}N signals can be clearly correlated with the corresponding ^{14}N signals and where the ^{13}C signals are strongly enhanced. Thus, the observation of ^{14}N $\Delta m_I = \pm 2$ signals at Q-band provides a new technique for examining weak interactions with a cluster. Six proteins show an additional pattern near $\nu \approx 18$ MHz that arises from ^{57}Fe in natural abundance (2.2%) with $A(^{57}Fe) \approx 36$ MHz, which opens the possibility of studying proteins for which enrichment is impractical. Q-band ENDOR studies also have been carried out on four ^2H-exchanged Fe–S proteins, and ENDOR detects exchangeable protons in each. The importance of these findings for the interpretation of X- and Q-band ENDOR at low radiofrequencies is discussed.

In this paper the benefits of performing ENDOR[1] experiments at higher microwave frequencies are demonstrated in a Q-band (35 GHz) ENDOR study of 10 proteins that contain [*n*Fe–*m*S] clusters, $n = 2, 3, 4$. In every case, the Q-band ENDOR spectra show proton resonances centered at $\nu(^1H) \approx 54$ MHz, but also a number of resonances in the range 0–20

† This work was supported by the National Institutes of Health (GM 34812 to H.B. and HL 13531 to B.M.H.) and the USDA (90-37120-5604 to B.M.H. and 88-37262-3406 to J.L.M.). It benefited from support by the Northwestern University Materials Research Center.
* Author to whom correspondence should be addressed.
‡ Northwestern University.
§ University of Wisconsin—Madison.
∥ Medical College of Wisconsin.

[1] Abbreviations: ENDOR, electron nuclear double resonance; EPR, electron paramagnetic resonance; ESEEM, electron spin echo envelope modulation; Fd, ferredoxin; HiPIP, high potential iron protein; NMR, nuclear magnetic resonance; RF, radio frequency; PDO, phthalate dioxygenase.

0006-2960/92/0431-2073$03.00/0

MHz. The appearance of such peaks at first is surprising, for in these proteins the ligands to the cluster Fe ions have no significant percentage of an isotope with nuclear spin $I > 0$. We show that a peak near $\nu \approx 13$ MHz seen for each protein can be assigned to natural-abundance ^{13}C nuclei (1.1%) so remote from the paramagnetic center that nuclear–nuclear dipole interactions are larger than electron–nuclear interactions, so-called "distant" ENDOR (Borghini, 1968; Borghini & Scheffler, 1971; Boroske & Möbius, 1977). A number of proteins also show resolved ^{13}C couplings [$A(^{13}C) \approx 1$ MHz] that are assigned to the β carbon of cluster-bound cysteine. A resonance near $\nu \approx 8$ MHz seen in all cases is assigned to nominally forbidden ^{14}N $\Delta m_I = \pm 2$ ENDOR transitions that arise from remote nitrogens. Spectra from five proteins further display $\Delta m_I = \pm 2$ ENDOR signals from local ^{14}N with isotropic hyperfine couplings of $0.4 \lesssim A(^{14}N) \lesssim 1.0$; these most likely are associated with N–H···S hydrogen bonds to the cluster. *Anabaena* 7120 Fd shows another signal corresponding to $A(^{14}N) \approx 4$ MHz. These interpretations are confirmed by examination of *Anabaena* Fd that has been enriched in ^{15}N or ^{13}C. Both local and distant ^{14}N signals can be used to derive the quadrupole coupling constant, as well as the hyperfine coupling. Thus, Q-band ENDOR provides a means of examining weak interactions that might be important in modifying the properties of an Fe–S cluster. Another set of weak resonances near $\nu \approx 18$ MHz is seen with five proteins and results from ^{57}Fe in natural abundance (2.2%), with $A(^{57}Fe) \approx 36$ MHz. This finding opens up the possibility that proteins for which iron enrichment is impractical can be studied in natural abundance. Q-band ENDOR studies have also been carried out on four ^2H-exchanged Fe–S proteins: the $[3Fe\text{-}4S]^+$ forms of hydrogenase and aconitase, the $[4Fe\text{–}4S]^+$ cluster of *Chromatium vinosum* HiPIP, and the $[2Fe\text{–}2S]^+$ cluster of *Anabaena* Fd. In each of these proteins ENDOR detects exchangeable protons.

The appearance of the ^{13}C and ^{14}N resonances has two further consequences. First, they may be misinterpreted, causing an incorrect assignment of resonances. Such was the case where similar ENDOR signals seen in a study of natural-abundance aconitase were attributed to strongly coupled ^{14}N (Werst et al., 1990). Second, the detection in numerous cases of a small isotropic hyperfine coupling to a ^{14}N that is not a ligand to a metal ion of a cluster proves that the presence of such a coupling to a cluster of unknown structure, such as the MoFe cofactor of nitrogenase or the H-cluster of hydrogenase I (Thomann et al., 1987, 1991), cannot, by itself, be used to infer the presence of ^{14}N directly coordinated to a metal ion. Nor, as we discuss, does the value of the coupling even provide a simple measure of the degree of covalency in the bond to the cluster.

Experimental Procedures and Theory

Sample Preparation. Samples of *Anabaena* Fd have been prepared with natural abundance ^{14}N and ^{13}C as well as with 40% uniform enrichment in ^{13}C. Another set of samples was grown on ^{15}N and is >95% pure in this nitrogen isotope as determined by NMR. Other Fe–S proteins employed are listed in Table I, and their purification is described in the references given therein.

Deuterium-exchanged aconitase was prepared by conversion to the purple form at pD 10.5 using solutions prepared with 99% D_2O as described (Kennedy et al., 1984). After incubating 24 h at room temperature, the solution was desalted on gels equilibrated with 0.1 M Hepes in D_2O, pD 7.5. The eluate was activated with Fe and DTT and was then converted to the [3Fe–4S] cubane form by ferricyanide oxidation (Kennedy et al., 1983). The method described by Backes et al. (1991) was used in the deuterium exchange of *C. vinosum* HiPIP and *Anabaena* Fd. The final dialysis step, however, was replaced by repeated washing and concentrating of the protein solution using the Centricon-10 ultrafiltration unit.

The high-potential Fe–S proteins were originally prepared in the laboratory of Drs. T. E. Meyer and M. A. Cusanovich of the University of Arizona, Tucson. Fd II of *Desulfovibrio gigas* was prepared by Drs. J. and I. Moura of the University of Lisbon, and spinach Fd and *Escherichia coli* fumarase were supplied by Dr. M. Emptage.

ENDOR Measurements. Q-band ENDOR spectra were recorded as described elsewhere (Gurbiel et al., 1989; Werst et al., 1991). As the emphasis of this work is on weak features

Table I: Hyperfine Coupling Constants (MHz)[a]

protein	^{14}N A	^{14}N K'	$A(^{13}C)$	$A(^{57}Fe)$
D. gigas hydrogenase $[3Fe\text{–}4S]^+$	d	1.7	d	40[b]
	0.7[c]	1.1		
actonitase $[3Fe\text{–}4S]^+$	d	1.4	d	36[b]
	0.4[c]	1.4		
aconitase $[4Fe\text{–}4S]^+$	d	1.1	d	
	0.4[c]	1.2		
E. coli fumarase A $[4Fe\text{–}4S]^+$	d	1.2	d	
Rhodospirillum tenue HiPIP $[4Fe\text{–}4S]^{3+}$	d	1.4	d	36[b]
C. vinosum HiPIP $[4Fe\text{–}4S]^{3+}$	d	1.5	d, 0.8, 1.4[e]	36[b]
E. halophila HiPIP $[4Fe\text{–}4S]^{3+}$	d	1.4	d, 0.8, 1.4[e]	36[b]
D. gigas Fd II $[4Fe\text{–}4S]^+$	d	1.5	d, 0.8, 1.4[e]	36[b]
spinach Fd $[2Fe\text{–}2S]^+$	d		1.0[e]	
	0.9[c]			
Anabaena Fd $[2Fe\text{–}2S]^+$	d	1.5	d, 1.2, 2.1[e]	
	1.0[c]	1.4		
	4.0[d]			
Pseudomonas cepacia phthalate dioxygenase[h] $[2Fe\text{–}2S]^+$	6.2[d]			
T. roseopersicina hydrogenase[i] $[3Fe\text{–}4S]^+$	1[f]			
D. gigas hydrogenase[j] $[3Fe\text{–}4S]^+$	1[f]			
milk xanthine oxidase[k] $[2Fe\text{–}2S]$	1[f]			
C. pasteurianum Fd[l] $[4Fe\text{–}4S]^{3+}$				$A_{x,y,z}$[g] = 33, 29, 25
E. coli fumarate reductase[m]	1.1[f]			
C. pasteurianum nitrogenase[n]	1.6[f]			

[a] d denotes the observation of distant ENDOR from ^{13}C ($\Delta m_I = \pm 1$) and ^{14}N ($\Delta m_I = \pm 2$). $K' = [K^2(3 + \eta)]^{1/2}$ is the ^{14}N quadrupole parameter. Hyperfine (A) and quadrupole (K') couplings are in MHz. Their uncertainties are A, ±10%; K', ±0.1 MHz. [b] Detected from ^{57}Fe in natural abundance. [c] Detected on $\Delta m_I = \pm 2$ transition of natural-abundance protein. [d] Detected on $\Delta m_I = \pm 1$ transition of natural-abundance protein. [e] Detected in natural-abundance protein and in ^{13}C-enriched *Anabaena* Fd. [f] Detected in ESEEM. [g] Detected by ENDOR on ^{57}Fe-enriched protein. [h] Isotropic component of ^{14}N hyperfine tensor (Gurbiel et al., 1989). [i] Cammack et al. (1988). [j] Chapman et al. (1988). [k] Cammack et al. (1991). [l] Anderson et al. (1975). [m] Cammack et al. (1988). [n] Thomann et al. (1987).

at low radio frequency (RF), special care was taken to ensure that none represented ^{1}H ENDOR transitions exicted by RF harmonics created in the PTS 160 synthesizer and/or ENI 3200L RF amplifier. Precautions included the use of an HP 8591A spectrum analyzer to measure the intensity of harmonics and, in selected controls, the use of a low-pass RF filter with attenuation of -60 dB above 45 MHz to eliminate harmonics near $\nu(^1\text{H}) \approx 54$ MHz. In all cases, reported spectra were taken with the filter on or at sufficiently low RF power that no features at low frequency could be attributed to ^{1}H harmonics.

We recall that for a single-crystal ENDOR measurement from a nucleus (or set of equivalent nuclei) J of spin I, one expects $4I$ transitions obeying the selection rules $\Delta m_S = 0$ and $\Delta m_I = \pm 1$. The transitions occur at frequencies given in first order by (Abragam & Bleaney, 1970)

$$\nu_\pm(m_I) = |\pm A^J/2 + \nu_J + 3P^J(2m_I - 1)| \quad (1)$$

where $-I + 1 < m_I < I$ and A^J and P^J are the angle-dependent hyperfine coupling and quadrupole constants, respectively, and ν_J is the nuclear Larmor frequency. In particular, the single-crystal spectrum of ^{14}N($I = 1$) consists of a doublet either centered at ν_N (3.845 MHz at 1.25 T) and split by A^N or centered at $A^N/2$ and split by $2\nu_N$. Each peak of the doublet may be further split into doublets by the quadrupolar interaction if there is sufficient resolution. In addition, state mixing by the quadrupole interaction for ^{14}N($I = 1$) (Cline et al., 1985) gives rise to $\Delta m_I = \pm 2$ transitions, with the maximum intensity in a powder sample expected at frequencies

$$\nu_{\pm 2} = 2[(\nu_N \pm A^N)^2 + K^2(3 + \eta^2)]^{1/2} \quad (2)$$

where $K = e^2qQ/4h = P_{max}/2$ is the quadrupole coupling constant and η is the asymmetry parameter (Dikanov & Astashkin, 1989; Flanagan & Singel, 1987). Equation 2 assumes A^N and $K \ll 2\nu_N$; exact simulations show that in this case eq 2 is accurate to better than the precision with which peaks can be measured.

^{15}N($I = {}^1/_2$), on the other hand, has no quadrupole interaction, and a ^{15}N spectrum is simply a doublet centered at ν_N or $A^N/2$, whichever is larger, and split by A^N or $2\nu_N$, whichever is smaller:

$$\nu_\pm = |\pm A^N/2 + \nu_N| \quad (3)$$

Because ^{1}H, ^{13}C, and ^{57}Fe all have $I = {}^1/_2$, their single-crystal spectra also follow eq 3. The magnitudes of the hyperfine coupling constants of ^{14}N and ^{15}N in different samples of the same protein are related to each other through

$$A(^{15}\text{N})/A(^{14}\text{N}) = |g(^{15}\text{N})/g(^{14}\text{N})| = \nu_N(^{15}\text{N})/\nu_N(^{14}\text{N}) \quad (4)$$

The samples employed in this study are frozen solutions, but ENDOR signals obtained at observing fields across the EPR envelope each result from select subsets of all possible orientations (Hoffman et al., 1984, 1989, 1991).

The center of a recorded ENDOR pattern often shifts in the direction of the radio-frequency sweep. To correct for this sweep artifact, the frequencies used in determining coupling constants were the average of peak positions measured in positive and negative scans.

Many of the ENDOR features, particularly those of ^{2}H and those associated with distant ENDOR, are quite asymmetric, rising sharply as the RF is swept into resonance, but having long tails as the RF sweeps on. This slow decay of the ENDOR intensity is well known to be associated with nuclear spin relaxation (Feher, 1959).

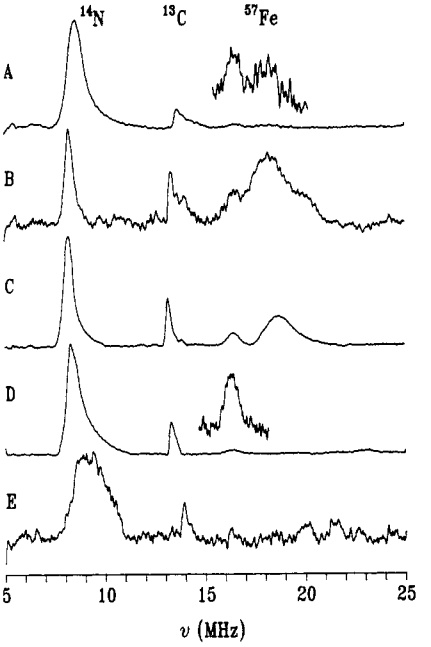

FIGURE 1: Q-band ENDOR of several natural abundance Fe–S proteins: (A) *D. gigas* Fd II; (B) *C. vinosum* HiPIP; (C) *E. halophila* HiPIP; (D) beef heart aconitase $[3Fe–4S]^+$ cluster; (E) beef heart aconitase $[4Fe–4S]^+$ cluster. Conditions: temperature, 2 K; modulation frequency, 100 kHz; radio frequency power, 25 W; radio frequency scan rate (RF), 1 MHz/s; time constant (TC), 0.032 s; microwave power (MWP): (A) 7.9, (B) 50, (C) 7.9, (D) 5, (E) 0.8 mW; microwave frequency (MWν): (A and B) 35.33, (C) 34.70, (D) 34.69, (E) 34.64 GHz; spectra were taken at g_2 with magnetic field (H): (A) 1.260, (B) 1.234, (C) 1.219, (D) 1.229, (E) 1.281 T; modulation amplitude (MA): (A–E) 0.8 mT; number of scans (NS): (A) 50, (B and C) 100, (D) 50, (E) 100.

Results

We have obtained Q-band ENDOR spectra from a variety of natural-abundance Fe–S protein samples. As noted in Table I, these include the $[3Fe–4S]^+$ and $[4Fe–4S]^+$ clusters of enzymes, the $[4Fe–4S]^{3+}$ clusters of high potential iron proteins (HiPIP's), and $[2Fe–2S]^+$ and $[4Fe–4S]^+$ ferredoxins. We first describe and interpret spectra from proteins in natural isotopic abundance. We then present data from the Fd of *Anabaena* 7120 labeled with ^{13}C and ^{15}N that confirm this interpretation.

^{13}C and ^{14}N ENDOR Resonances. Figure 1 shows representative low-frequency Q-band ENDOR spectra from proteins with Fe–S clusters. Each was taken at the field of greatest intensity in the EPR envelope. These spectra all show peaks at ~9 and ~13 MHz. Because proton resonances occur near $\nu(^1\text{H}) \approx 53$ MHz and the samples are isotopically unenriched, the peaks might plausibly be taken to be ^{14}N resonances. If one assumes that the observed resonances are the first order, $\Delta m_I = \pm 1$, transitions described by eq 1, these two peaks cannot be a $\nu_\pm$ pair centered at an average frequency of $A(^{14}\text{N})/2 \approx 11$ MHz. Such a pair should be split by $\nu_+ - \nu_- = 2\nu(^{14}\text{N}) \approx 8$ MHz, whereas the actual splitting is significantly smaller.

Alternatively, if these peaks are each ν_+ resonances from different ^{14}N sites, the ν_- partners would appear below 5 MHz where they might not be detected. In every case, this latter interpretation would give $A(^{14}\text{N1}) \approx 18$ and $A(^{14}\text{N2}) \approx 10$ MHz (eq 1), suggesting direct ligation of N to the cluster. However, for none of these proteins is there evidence that any amino acid other than cysteine ligates the Fe atoms of any of the clusters (no amino acid is ligated to the aconitase cluster except Cys), and furthermore, the crystal structures of aco-

nitase, *D. gigas* Fd II, and *C. vinosum*, and *Ectothiorhodospira halophila*[2] HiPIP's confirm this conclusion (Rypniewski et al., 1991; Backes et al., 1991; Robbins & Stout, 1989). Couplings of 18 or even 10 MHz are exceptionally large for noncoordinate nitrogen. For comparison, note that the largest ^{14}N hyperfine coupling constant in phthalate dioxygenase, where the nitrogens are coordinated to the [2Fe–2S] cluster, is 7.0 MHz (Gurbiel et al., 1989). Clearly, this assignment to ν_+ resonances is unacceptable because it would imply unusually large hyperfine constants and because it is improbable that peaks would appear in the same positions in each of the different proteins.

At the external magnetic field employed in collecting each of these spectra, the Larmor frequency for ^{13}C is $\nu(^{13}C) \approx 13$ MHz. Thus, a more reasonable interpretation of the resonances near 13 MHz is that they represent distant ENDOR signals from ^{13}C in natural abundance (1.1%) (Pilbrow, 1990; Böttcher et al., 1985; Boroske & Möbius, 1977) with apparent discrepancies from the value of $\nu(^{13}C)$ deriving from the sweep artifact (see Experimental Procedures and Theory). Detailed examination of the ^{13}C signals (data not shown) confirms an impression given by Figure 1 that a number of proteins also show local ENDOR peaks with two distinct couplings, $A(^{13}C) \approx 1$ MHz, seen in each case (Table I). These must result from coupling to the β carbons of cysteine coordinated to the cluster; the two resolved couplings likely are associated with ligands to different iron ions. These assignments are confirmed below in the discussion of natural-abundance and ^{13}C-enriched *Anabaena* Fd.

For each of the spectra in Figure 1, the strongest peak falls near $2\nu(^{14}N)$, which is 7.69 MHz at 1.25 T, leading us to assign these peaks to $\Delta m_I = \pm 2$ transitions of ^{14}N (eq 2); this assignment is confirmed by the field dependence of the spectra and by ^{15}N substitution in *Anabaena* Fd (see below). Because the $\Delta m_I = \pm 2$ signals are without hyperfine splitting [eq 2, $A(^{14}N) = 0$] and are rather narrow, they most likely represent a distant ^{14}N signal. Even after correction for the sweep artifact (vide supra), the $\Delta m_I = \pm 2$ frequency is consistently greater than $2\nu(^{14}N)$. This frequency can be used with eq 2 to derive the effective quadrupole coupling, $K' \equiv K(3 + \eta^2)^{1/2}$, for the distant ^{14}N; values of K' in the range 1.1–1.5 MHz are obtained for the entire set of proteins studied (Table I). In addition to the distant ^{14}N signals, the $\Delta m_I = \pm 2$ peaks for the $[3Fe–4S]^+$ and $[4Fe–4S]^+$ clusters of aconitase, the $[3Fe–4S]^+$ cluster of *D. gigas* hydrogenase, and the $[2Fe–2S]^+$ cluster of spinach Fd further show peaks split by a local ^{14}N hyperfine coupling ($0.4 \lesssim A(^{14}N) \lesssim 1$ MHz; Table I) that is not resolved under the conditions employed in Figure 1 (data not shown); such hyperfine splitting is seen for the *Anabaena* Fd (Figure 3), and it is discussed below. Similar ^{14}N hyperfine couplings have been observed frequently in ESEEM studies on Fe–S clusters, such as those of *Thiocapsa roseopersicina* (Cammack et al., 1989) and *D. gigas* hydrogenase (Chapman et al., 1985), *E. coli* fumarate reductase (Cammack et al., 1988), and milk xanthine oxidase (Cammack et al., 1991). For comparison representative cases are listed in Table I.

As $\Delta m_I = \pm 2$ transitions for distant ^{14}N are clearly observed in Figures 1 and 2, one might also expect to see the corresponding $\Delta m_I = \pm 1$ transitions. With $A(^{14}N) \approx 0$, however, these transitions should be in resonance at $\nu(^{14}N) = 4$ MHz. It is likely that they typically do not appear in the Q-band spectra (data not shown) because such low-frequency peaks are difficult to observe. Because the intensities of the $\Delta m_I = \pm 2$ transitions vary as $[P/(\nu_N \pm A^N/2)]^2 \approx [P/\nu_N]^2$, they are normally expected to be stronger at the lower microwave frequencies of X-band. However, these transitions are not usually seen at this frequency even though they are quite obvious in the present Q-band study. The most likely reason is that at the magnetic field for $g = 2$ in X-band the $\Delta m_I = \pm 2$ transitions occur at $2\nu(^{14}N) = 2$ MHz and are difficult to detect at such a low frequency.

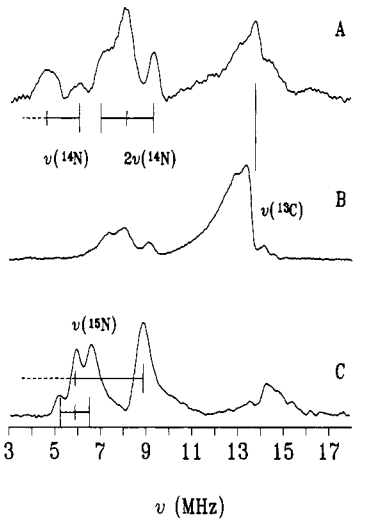

FIGURE 2: ENDOR of *Anabaena* 7120 Fd: (A) natural abundance; (B) 40% ^{13}C-enriched; (C) >90% ^{15}N-enriched. Connecting bars indicate $\nu_\pm$ or $\nu_{\pm 2}$ partners. Conditions are as described for Figure 1E except for the following: RF; (A, B, and C) 0.5; TC, (A) 0.128, (B) 0.032, (C) 0.064 s; MWP, 0.5 mW; MWν, (A) 34.68, (B) 34.67, (C) 34.72 GHz; H (g_2), (A) 1.308, (B and C) 1.268 T; MA, 4 mT; NS, (A) 20, (B) 5, (C) 50. Spectra A and B were taken with a negative RF sweep.

Finally, every spectrum in Figure 1 with the exception of the [4Fe–4S] cluster of aconitase (Figure 1E) shows resonances near 18 MHz that can be attributed to natural-abundance ^{57}Fe (2.2%). This implies that these different Fe–S clusters all have Fe sites with hyperfine couplings, $A(^{57}Fe) \approx 36$ MHz (eq 3). Comparable ^{57}Fe couplings have been seen, for example, with Mössbauer spectroscopy (Surerus et al., 1989) and in ENDOR studies of ^{57}Fe-enriched aconitase (Werst et al., 1990), *C. vinosum* HiPIP, and *Clostridium pasteurianum* Fd (Anderson et al., 1974; Sands, 1979) (Table I). For proteins such as the *C. vinosum* (Figure 1B) and *E. halophila* (Figure 1C) HiPIP's, the ^{57}Fe ENDOR intensity is adequate to perform complete analysis of the ^{57}Fe hyperfine tensor(s).

$[2Fe–2S]^+$ Cluster of Anabaena Fd. To test the above assignment of resonances in the Fe–S proteins, extensive ENDOR studies were done on the $[2Fe–2S]^+$ cluster of *Anabaena* Fd. This protein was chosen because its crystal structure shows that no nitrogenous ligand is coordinated to the cluster (Rypniewski et al., 1991) and because ^{15}N- and ^{13}C-enriched samples were available for comparison to samples with natural-abundance ^{14}N and ^{13}C.

An ENDOR spectrum at $g = 1.894$ of natural-abundance *Anabaena* Fd is shown in Figure 2A. Consistent with the observations on all the other Fe–S proteins (Figure 1), there is a peak near 14 MHz, corresponding to $\nu(^{13}C)$, that we attribute to natural-abundance ^{13}C. This assignment is confirmed by the ENDOR spectrum of a sample of *Anabaena* Fd enriched to 40% in ^{13}C. In this spectrum (Figure 2B) a large asymmetric (see Experimental Procedures and Theory) ^{13}C peak dwarfs all other features. The position of this large resonance also coincides with the ^{13}C Larmor frequency, $\nu(^{13}C)$

[2] Private communication from H. M. Holden.

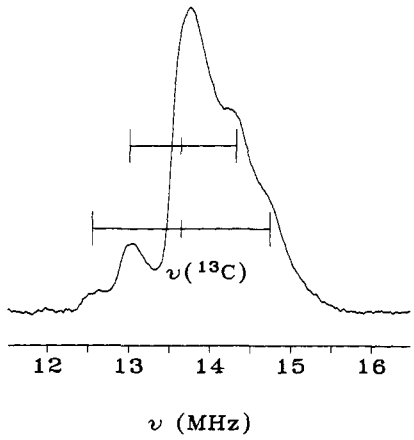

FIGURE 3: ENDOR of ^{13}C-enriched *Anabaena* Fd. Connecting bars indicate ν_+ and ν_- partners. Conditions are as described for Figure 1E except for the following: RF, 0.25 MHz/s; TC, 0.064 s; MWP, 0.5 mW; MWν, 34.68 GHz; H, 1.268 T; MA; 0.5 mT; NS, 50.

= 13.6 MHz. The field dependencies of the 14 MHz peaks for both the ^{13}C-enriched and the unenriched samples closely correspond to the field dependence of the ^{13}C Larmor frequency (data not shown), confirming that the signal at $\nu(^{13}C)$ in unenriched *Anabaena* Fd and, by inference, in the other proteins represents distant ^{13}C ENDOR.

The spectrum from the ^{13}C-enriched sample also exhibits resolved local ENDOR signals (Figure 3) that correspond to two hyperfine-split doublets centered at $\nu(^{13}C)$ (eq 3). The hyperfine coupling constants of these two doublets are somewhat anisotropic, but because of the strong overlap, the exact tensor of each is difficult to determine. The range of the two hyperfine coupling constants observed throughout the EPR envelope is as follows: $A(^{13}C1)$ = 0.76–1.2 and $A(^{13}C2)$ = 1.9–2.1 MHz. The detected carbon nuclei are undoubtedly those of the cysteine side chains, bonded through S to an Fe of the $[2Fe–2S]^+$ cluster.

In addition to the ^{13}C peak in the spectrum of unenriched *Anabaena* Fd (Figure 2A), there are three features centered near $2\nu(^{14}N) \approx 8.0$ MHz that we may assign to the $\Delta m_I = \pm 2$ transitions of nitrogen. The center peak presumably can be assigned to distant nitrogen [$A(^{14}N)_{dist} \approx 0$], and the flanking doublet corresponds to $\nu_{\pm 2}$ peaks of a local nitrogen, N1. The frequency of the center, distant ENDOR peak, when used with eq 2, gives an effective quadrupole contribution $K' = K(3 + \eta^2)^{1/2} \approx 1.5$ MHz. The positions of the local ^{14}N doublet peaks give $A(^{14}N1)$ = 1.0 MHz and K' = 1.5 MHz. Figure 4 shows the field dependence of both distant and local ^{14}N $\Delta m_I = \pm 2$ transitions of *Anabaena* Fd, along with the peak positions calculated using the above parameters in eq 2. The match is well within experimental error and confirms the analysis as $\Delta m_I = \pm 2$ resonances.

Figure 2A also shows weak features in the range 4–6.5 MHz that appear to be $\Delta m_I = \pm 1$ transitions for ^{14}N. One such peak occurs near $\nu(^{14}N) \approx 4$ MHz and could result from the $\Delta m_I = \pm 1$ transitions of the same nitrogen sites that give rise to the $\Delta m_I = \pm 2$ peak. There is another weak feature at 6.0 MHz that might be the ν_+ peak of a hyperfine-split local-ENDOR doublet centered at $\nu(^{14}N)$ and corresponding to an isotropic hyperfine coupling constant $A(^{14}N2) \approx 4.0$ MHz.

The above interpretation of the spectrum of natural-abundance *Anabaena* Fd involves three types of ^{14}N sites: distant ^{14}N with $A(^{14}N_{dist}) \approx 0$; those with $A(^{14}N1) \approx 1.0$; and those with $A(^{14}N2) \approx 4.0$ MHz. According to eq 4, in the ^{15}N-enriched protein these sites should have hyperfine coupling constants of $A(^{15}N_{dist}) \approx 0$, $A(^{15}N1) \approx 1.4$, and $A(^{15}N2) \approx$

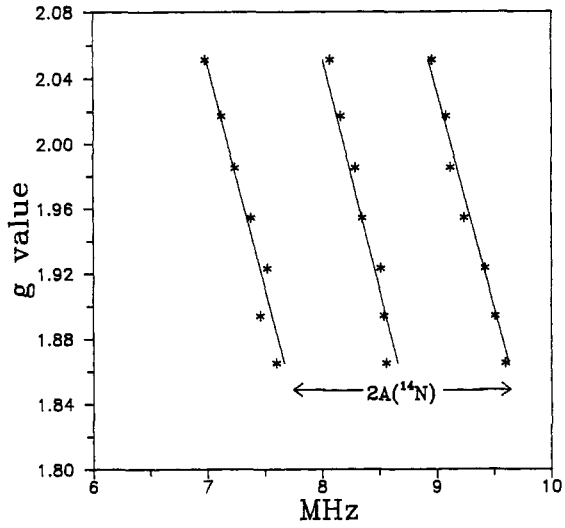

FIGURE 4: Plot of average peak position in MHz of ^{14}N $\Delta m_I = \pm 2$ transitions vs observing g value for natural-abundance *Anabaena* Fd MWν = 34.68 GHz. Solid lines represent peak positions calculated from eq 2. For the center (distant) peak, A^N = 0 and $K^2(3 + \eta^2)$ = 2.2 MHz; for the flanking doublet, A^N = 1.0 MHz and $K^2(3 + \eta^2)$ = 2.0 MHz.

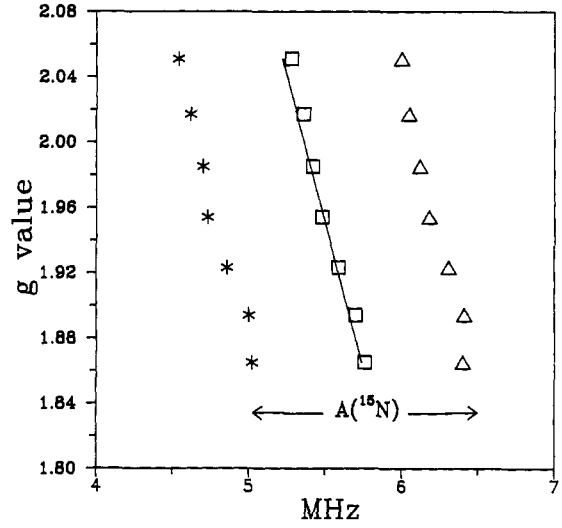

FIGURE 5: Plot of average peak positions in MHz of ^{15}N $\Delta m_I = \pm 1$ transitions vs observing g value for ^{15}N-enriched *Anabaena* Fd: (Δ) ν_+ peak; (*) ν_- peak for local ^{15}N ENDOR with $A(^{15}N)$ = 1.5 MHz; distant ENDOR (□) peak. The solid line follows the Larmor frequency of ^{15}N: MWν = 34.72 GHz.

5.6 MHz. The ENDOR spectrum of this protein should then show a $\Delta m_I = \pm 1$ pattern centered at $\nu(^{15}N)$ = 5.6 MHz with a feature at $\nu(^{15}N)$ for distant nitrogens and hyperfine-split doublets for N1 and N2 (eq 3). The low-frequency ENDOR spectrum for ^{15}N-enriched *Anabaena* Fd in Figure 2C confirms these predictions. Furthermore, Figure 5 shows that the field dependence of the N1 signal follows that of $\nu(^{15}N)$ as predicted by eq 3 if N1 has an isotropic hyperfine interaction. Figure 2C also shows a strong resonance at 8.6 MHz. This falls near the frequency of the ^{14}N $\Delta m_I = \pm 2$ transition, but the assignment of this peak to the $\Delta m_I = \pm 2$ transition is unacceptable because it is as intense as $\Delta m_I = \pm 2$ transitions from ^{14}N in natural abundance (99.6%); yet the residual ^{14}N in this ^{15}N-enriched sample of *Anabaena* Fd is less than 5% as determined by NMR. As a result, the peak is better assigned to ^{15}N, namely, the ν_+ peak of a hyperfine-split doublet with $A(^{15}N2) \approx 6.0$ MHz, in agreement with the prediction from the ^{14}N results. The ν_- peak would occur at 2.6 MHz and is

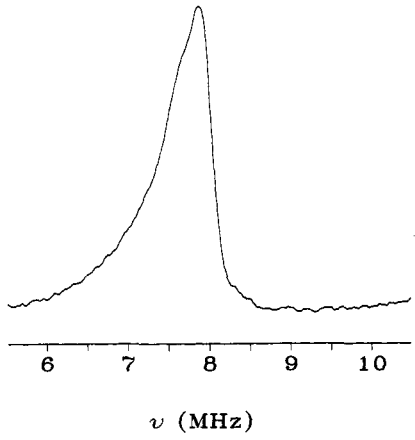

FIGURE 6: ENDOR of ^2H_2O-exchanged aconitase $[3Fe–4S]^+$ cluster. Conditions are as in Figure 1E except for the following: RF, 0.2 MHz/s; TC, 0.128 s; MWP, 0.5 mW; MWν, 34.72 GHz; H, 1.232 T; MA, 0.1 mT; NS, 100. The spectrum was taken with a negative RF sweep.

not detected, presumably because of its low frequency. The complete field dependence of the ^{15}N sample (data not shown) indicates that the hyperfine tensor of this nitrogen site also is essentially isotropic. Such a hyperfine coupling constant appears large for a noncoordinated nucleus—again compare $A_{max}(^{15}N)$ = 9.8 MHz from a coordinated nitrogen of phthalate dioxygenase (PDO) (Gurbiel et al., 1989)—and thus may reflect weak coordination as a fifth ligand to the $[2Fe–2S]^{1+}$ cluster, as opposed to hydrogen bonding. However, we note such direct comparisons can be misleading. The coordinated nitrogens in PDO are bound to the Fe(II) site, whereas the most likely residue to be involved in secondary interactions with the cluster in *Anabaena* Fd, Arg 42, interacts more strongly with the Fe(III) site (Skjeldal et al., 1991). It is easy to show that in the latter case a given spin density on nitrogen gives an observed hyperfine coupling that is a factor of (35/16) larger than in the former.

^1H and ^2H ENDOR Studies. Deuterium exchange procedures have been performed on $[3Fe–4S]^+$ aconitase, $[4Fe–4S]^{3+}$ HiPIP from *C. vinosum*, $[3Fe–4S]^+$ hydrogenase from *D. gigas*, and *Anabaena* Fd to examine the possibility that the nitrogens of nearby amino acids form hydrogen bonds with the Fe–S cluster. The ^1H ENDOR spectrum of each of these proteins exhibits numerous hyperfine-split doublets from protons with $0 < A < 12$ MHz. In no case does exchange lead to the loss of a proton with large coupling, $A(^1H) \geq 4$ MHz [compare Chapman et al. (1988)], and it is difficult to be certain about exchange of protons with smaller couplings.

In the case of a ^2H-exchanged sample of aconitase, however, an intense ^2H resonance appeared, centered at $\nu(^2H)$ (Figure 6). As estimated by the half-width from the rising portion of the ^2H resonance, the hyperfine coupling constant(s) must have value(s) $A(^2H) < 0.5$ MHz. Note, however, the peak exhibits weak structure that probably is due to a local hyperfine coupling, $A(^2H) \sim 0.2$ MHz. Similar ^2H ENDOR signals were obtained from ^2H-exchanged *C. vinosum* HiPIP, the *D. gigas* hydrogenase $[3Fe–4S]^+$ cluster, and *Anabaena* Fd. Whether these are in part local ENDOR signals with $A(^2H) \neq 0$ or entirely distant ENDOR responses with $A(^2H) \approx 0$ cannot be determined here. Pulsed ENDOR studies are being used to address this issue (Fan et al., 1991).

DISCUSSION

All the Fe–S proteins studies here show distant ENDOR resonances from ^{14}N and ^{13}C in natural abundance. The $^{13}C(I = {}^1/_2)$ signal is seen as a single line at the Larmor frequency. The $^{14}N(I = 1)$ resonance is seen as a line at $2\nu(^{14}N)$ and is attributed to a nominally forbidden $\Delta m_I = \pm 2$ transition that is allowed by the ^{14}N quadrupole interaction. These assignments are confirmed by our studies of natural-abundance, ^{13}C-enriched, and ^{15}N-enriched *Anabaena* Fd. Several proteins also show local ^{13}C ENDOR that is assigned to the β carbons of cluster-bound cysteine, as well as resonances from ^{57}Fe in natural abundance (Table I).

Anabaena Fd, the $[3Fe–4S]^+$ and $[4Fe–4S]^+$ clusters of aconitase, the $[3Fe–4S]^+$ cluster of *D. gigas* hydrogenase, and spinach Fd also show ^{14}N resonances with resolved hyperfine splitting from local ENDOR. These five proteins each have one resolved nitrogen with a small local coupling of $A(^{14}N) \leq 1.0$ MHz, and *Anabaena* Fd has a second nitrogen with a larger coupling, $A(^{14}N) \approx 4.0$ MHz, as confirmed by the results from the ^{15}N-enriched protein. These nitrogen resonances have essentially isotropic hyperfine tensors, indicating that the predominant mechanism of coupling is a covalent interaction. There have been numerous ESEEM measurements for clustes where ^{14}N resonances were detected with quadrupole splitting and weak hyperfine coupling comparable to those seen in our studies [for example, see Peisach et al. (1977), Lo Brutto et al. (1987), Mims and Peisach (1989), Cammack et al. (1988, 1989, 1991), and Chapman et al. (1988)]. Selected results are presented in Table I, along with those of the Fe–S proteins examined here.

At least two types of interactions might explain a small isotropic hyperfine coupling [$A(^{14}N) \sim 1$ MHz] to nitrogen that is not directly coordinated to an iron ion of a [nFe–mS] cluster. The nitrogen nuclei could interact via hydrogen bonding to an inorganic sulfide or cysteine sulfur of the cluster, or the coupling could proceed through the carbon chain of the cysteine residues that coordinate that Fe–S cluster to their backbone nitrogens. Oh and Markley (1990) have observed hyperfine-shifted ^{15}N signals in NMR and have invoked the latter explanation.

Cammack, on the other hand, has invoked hydrogen bonding to explain the observation of ^2H and ^{14}N hyperfine coupling in xanthine oxidase (Cammack et al., 1991) and fumarate reductase (Cammack et al., 1988). Evidence for hydrogen bonding to Fe–S clusters is provided by resonance Raman and crystallographic studies (Backes et al., 1991) and by NMR studies of *E. halophila* HiPIP's I and II, in which exchangeable protons are hyperfine shifted (Markley et al., 1986), and of *Peptococcus aerogenes* Fd, in which exchangeable protons bonded to nitrogen shift considerably upon reduction (Adman et al., 1975). In aconitase, several amino acids are well positioned to yield such NH···S bonds, particularly Asn 446 and Asn 228, both of which have highly favorable angles and distances from the cluster (C. D. Stout, private communication). The ^2H_2O exchange studies on *Anabaena* Fd, *D. gigas* hydrogenase, and the $[3Fe–4S]^+$ form of aconitase lend tentative support to a hydrogen-bonding explanation for the weakly coupled nitrogens. Further investigation in this area is planned.

The observation of ^{14}N $\Delta m_I = \pm 2$ transitions in each member of this set of proteins has consequences for the interpretation of spectra at both X-band and Q-band. First, the features with $\nu < 20$ MHz seen in the Q-band ENDOR spectra for the $[4Fe–4S]^+$ cluster of aconitase now can be assigned to ^{14}N $\Delta m_I = \pm 2$ and ^{13}C $\Delta m_I = \pm 1$ distant ENDOR transitions, and not to local ENDOR from nuclei having a large hyperfine coupling (Werst et al., 1990). Second, the observation in numerous cases of a small isotropic hyperfine

coupling to ^{14}N that is not a ligand to the metal ion of a cluster clearly proves that the observation of such a coupling in a cluster of unknown character, as with the molybdenum–iron cofactor of nitrogenase (Thomann et al., 1987; Table I) or the H-cluster of Fe-hydrogenase I (Thomann et al., 1991), does *not* necessarily imply the presence of direct nitrogen coordination to a metal ion.

Indeed, when considering a multimetal cluster, without a detailed understanding of spin coupling within the cluster, the ^{14}N hyperfine coupling does not *by itself* even provide a meaningful measure of the degree of covalency in the bond to the cluster, regardless of whether that bond involves coordination to a metal ion or hydrogen bonding to sulfur. As is well known, the observed hyperfine coupling is related to the spin density on nitrogen (or any other nucleus) by a proportionality constant that is determined by the spin-coupling scheme within the cluster (Kent et al., 1980; Werst et al., 1990). Thus, as noted above, a given spin density on nitrogen gives rise to a roughly 2-fold difference in observed hyperfine coupling, depending on whether the nitrogen interacts with the Fe(II) or Fe(III) site of a [2Fe–2S] cluster. The problem is even worse with larger clusters: a small spin density on nitrogen can give a disproportionately large observed coupling, whereas a large spin density can give a vanishingly small coupling! Indeed, we further note that the inorganic sulfide ions that form an integral part of the aconitase $[4Fe–4S]^+$ cluster give quite small hyperfine couplings (Werst et al., 1990).

Acknowledgments

The high-potential Fe–S proteins were kindly supplied by Drs. T. E. Meyer and M. A. Cusanovich of the University of Arizona, Tucson, or through the courtesy of Dr. H. Holden of the University of Wisconsin—Madison. Fd II of *D. gigas* was supplied by Drs. J. and I. Moura of the University of Lisbon, and spinach Fd and *E. coli* fumarase were supplied by Dr. M. Emptage. We are grateful to these colleagues for providing us with this material. In addition, we gratefully acknowledge the technical assistance of Clark Davoust.

Registry No. Hydrogenase, 9079-91-8; aconitase, 9024-25-3; fumarase, 9032-88-6; phthalate dioxygenase, 63626-44-8; xanthine oxidase, 9002-17-9; fumarate reductase, 9076-99-7; nitrogenase, 9013-04-1.

References

Abragam, A., & Bleaney, B. (1970) *Electron Paramagnetic Resonance of Transition Ions*, pp 43 and 91, Dover Publications, Inc., New York.

Adman, E., Watenpaugh, K. D., & Jensen, L. H. (1975) *Proc. Natl. Acad. Sci. U.S.A. 72*, 4854–4858.

Anderson, R. E., Anger, G., Peterson, L., Ehrenberg, A., Cammack, R., Hall, D. O., Mullinger, R., & Rao, K. K. (1974) *Biochim. Biophys. Acta 376*, 63–71.

Backes, G., Mino, Y., Loehr, T. M., Meyer, T. E., Cusanovich, M. A., Sweeney, W. V., Adman, E. T., & Sanders-Loehr, J. (1991) *J. Am. Chem. Soc. 113*, 2055–2064.

Borghini, M. (1968) *Phys. Lett. 26A*, 242–244.

Borghini, M., & Scheffler, K. (1971) *Nucl. Instrum. Methods 95*, 93–98.

Boroske, E., & Möbius, K. (1977) *J. Magn. Reson. 28*, 325–338.

Böttcher, R., Kirmse, R., Stach, J., & Keijzers, C. P. (1985) *Mol. Phys. 55*, 1431–1445.

Cammack, R., Chapman, A., McCracken, J., Cornelius, J. B., Peisach, J., & Weiner, J. H. (1988) *Biochim. Biophys. Acta 956*, 307–312.

Cammack, R., Kovacs, K. L., McCracken, J., & Peisach, J. (1989) *Eur. J. Biochem. 182*, 363–366.

Cammack, R., Chapman, A., McCracken, J., & Peisach, J. (1992) *J. Chem. Soc., Faraday Trans.* (in press).

Chapman, A., Cammack, R., Hatchikian, C. E., McCracken, J., & Peisach, J. (1988) *FEBS Lett. 242*, 134–138.

Cline, J. F., Janick, P. A., Siegel, L. M., & Hoffman, B. M. (1985) *Biochemistry 24*, 7942–7947.

Dikanov, S. A., & Astashkin, A. V. (1989) in *Advanced EPR: Applications in Biology and Biochemistry* (Hoff, A. J., Ed.) pp 59–117, Elsevier, Amsterdam.

Fan, C., & Hoffman, B. M. (1992) *J. Am. Chem. Soc. 114*, 374–375.

Feher, G. (1959) *Phys. Rev. 114*, 1219–1244.

Flanagan, H. L., & Singel, D. J. (1987) *J. Chem. Phys. 89*, 5606–5616.

Gurbiel, R. J., Batie, C. J., Sivaraja, M., True, A. E., Fee, J. A., Hoffman, B. M., & Ballou, D. P. (1989) *Biochemistry 28*, 4861–4871.

Hoffman, B. M. (1991) *Acc. Chem. Res. 24*, 164–170.

Hoffman, B. M., Martinsen, J., & Venters, R. (1984) *J. Magn. Reson. 59*, 110–123.

Hoffman, B. M., Gurbiel, R. J., Werst, M. M., & Sivaraja, M. (1989) in *Advanced EPR: Applications in Biology and Biochemistry* (Hoff, A. J., Ed.) pp 541–591, Elsevier, Amsterdam.

Kennedy, M. C., Emptage, M. H., Dreyer, J.-L., & Beinert, H. (1983) *J. Biol. Chem. 258*, 11098–11105.

Kennedy, M. C., Kent, T. A., Emptage, M., Merkle, H., Beinert, H., & Münk, E. (1984) *J. Biol. Chem. 259*, 14463–14471.

Kent, T. A., Huynh, B. H., & Münck, E. (1980) *Proc. Natl. Acad. Sci. U.S.A. 77*, 6574–6576.

Lo Brutto, R., Haley, P. E., Yu, C., & Ohnishi, T. (1987) in *Advances in Membrane Biochemistry and Bioenergetics* (Kim, C. H., Tedeschi, H., Diwan, J. J., & Salerno, J. C., Eds.) pp 449–458, Plenum, New York.

Markley, J. L., Chan, T.-M., Krishnamoorthi, R., & Ulrich, E. L. (1986) in *Iron–Sulfur Protein Research* (Matsubara et al., Eds.) pp 167–181, Japan Science Society Press, Tokyo/Springer-Verlag, Berlin.

Mims, W. B., & Peisach, J. (1989) in *Advanced EPR: Applications in Biology and Biochemistry* (Hoff, A. J., Ed.) pp 59–117, Elsevier, Amsterdam.

Oh, B.-H., & Markley, J. L. (1990) *Biochemistry 29*, 4012–4017.

Peisach, J., Orme-Johnson, N. R., Mims, W. B., & Orme-Johnson, W. H. (1977) *J. Biol. Chem. 252*, 5643–5650.

Pilbrow, J. R. (1990) *Transition Ion Electron Paramagnetic Resonance*, p 406, Oxford University Press, Oxford.

Robbins, A. H., & Stout, C. D. (1989) *Proc. Natl. Acad. Sci. U.S.A. 86*, 3639–3643.

Rypniewski, W. R., Breiter, D. R., Benning, M. M., Wesenberg, G., Oh, B.-H., Markley, J. L., Rayment, I., & Holden, H. M. (1991) *Biochemistry 30*, 4126–4131.

Sands, R. H. (1979) in *Multiple Electron Resonance Spectroscopy* (Dorio, M. M., & Freed, J. H., Eds.) pp 331–374, Plenum Press, New York.

Skjeldal, L., Westler, W. M., Oh, B.-H., Krezel, A. M., Holden, H. M., Jacobson, B. L., Rayment, I., & Markley, J. L. (1991) *Biochemistry 30*, 7363–7368.

Surerus, K. K., Kennedy, M. C., Beinert, H., & Münck, E. (1989) *Proc. Natl. Acad. Sci. U.S.A. 86*, 9846–9850.

Thomann, H., Morgan, T. V., Jin, H., Burgmayer, S. J. N., Bare, R. E., & Stiefel, E. I. (1987) *J. Am. Chem. Soc. 109*, 7913–7914.
Thomann, H., Bernardo, M., & Adams, M. W. W. (1991) *J. Am. Chem. Soc. 113*, 7044–7046.
Werst, M. M., Kennedy, M. C., Houseman, A. L. P., Beinert, H., & Hoffman, B. M. (1990) *Biochemistry 29*, 10533–10540.
Werst, M. M., Davoust, C. E., & Hoffman, B. M. (1991) *J. Am. Chem. Soc. 113*, 1533–1538.

Importance of Size and Sulfation of Heparin in Release of Basic Fibroblast Growth Factor from the Vascular Endothelium and Extracellular Matrix†

Rivka Ishai-Michaeli,‡ Carl M. Svahn,§ Michael Weber,§ Tova Chajek-Shaul,‖ Gil Korner,‡ Hans-Peter Ekre,§ and Israel Vlodavsky*,‡

Departments of Oncology and Medicine B, Hadassah University Hospital, Jerusalem 91120, Israel, and R & D Cardiovascular, Kabi Pharmacia, Stockholm S-11287, Sweden

Received July 5, 1991; Revised Manuscript Received November 12, 1991

ABSTRACT: We have characterized the importance of size, sulfation, and anticoagulant activity of heparin in release of basic fibroblast growth factor (bFGF) from the subendothelial extracellular matrix (ECM) and the luminal surface of the vascular endothelium. For this purpose, ^{125}I-bFGF was first incubated with ECM and confluent endothelial cell cultures, or administered as a bolus into the blood of rats. the immobilized ^{125}I-bFGF was then subjected to release by various chemically modified species of heparin and size-homogeneous oligosaccharides derived from depolymerized heparin. Both totally desulfated and N-desulfated heparin failed to release the ECM-bound bFGF. Likewise, substitution of *N*-sulfate groups of heparin and low molecular weight heparin (fragmin) by acetyl or hexanoyl residues resulted in an almost complete inhibition of bFGF release by these polysaccharides. The presence of *O*-sulfate groups in heparin increased but was not critical for release of ECM-bound bFGF. Similar structural requirements were identified for release of ^{125}I-bFGF bound to low-affinity sites on the surface of vascular endothelial cells. Oligosaccharides derived from depolymerized heparin and containing as little as 8–10 sugar units were, on a weight basis, equivalent to whole heparin in their ability to release bFGF from ECM. Low-sulfate oligosaccharides were less effective releasers of bFGF as compared to medium- and high-sulfate fractions of the same size oligosaccharides. Heparin fractions with high and low affinity to antithrombin III exhibited a similar high bFGF-releasing activity despite a 200-fold difference in their anticoagulant activities. Studies on the fate of intravenously administered ^{125}I-bFGF demonstrated that bFGF sequestered by the luminal surface of the vascular endothelium is accessible to release by heparin species in a manner similar to that observed for release of ECM-bound bFGF. Analysis of the distribution of ^{125}I-bFGF in various organs revealed the presence of intact ^{125}I-bFGF primarily in the rat liver and kidneys. Structural requirements for release of ECM-bound and cell-surface-bound bFGF by heparin and heparin-like molecules were different from those identified for inhibition of heparanase activity and lung colonization of B16 melanoma cells by these heparin molecules. These results indicate that various non-anticoagulant species of heparin having different size, sulfation, and substituted groups can be designed to elicit specific effects such as release of bFGF and inhibition of heparanase and hence for induction of neovascularization and inhibition of tumor metastasis, respectively.

Fibroblast growth factors (FGFs)[1] are a family of structurally related polypeptides characterized by high affinity to heparin (Burgess & Maciag, 1989; Gospodarowicz et al., 1987; Rifkin & Moscatelli, 1989). They are highly mitogenic for vascular endothelial cells (EC) and are among the most potent inducers of neovascularization and mesenchyme formation (Folkman & Klagsbrun, 1987; Kimelman & Kirschner, 1987). Among the FGF gene family are the prototypes acidic FGF (aFGF) and basic FGF (bFGF) which, unlike most other polypeptide growth factors, are primarily cell-associated, consistent with the lack of a conventional signal sequence for secretion (Burgess & Maciag, 1989; Gospodarowicz et al., 1987; Rifkin & Moscatelli, 1989). Despite the lack of a signal peptide, both aFGF and bFGF have been identified in the extracellular matrix (ECM) deposited by cultured myoblasts (Weiner & Swain, 1989) and EC (Baird & Ling, 1987; Vlodavsky et al., 1987). Immunohistochemical staining re-

† This work was supported by U.S. Public Health Service Grant CA30289 awarded to I.V. by the National Cancer Institute, DHHS, and by grants from the USA–Israel Binational Science Foundation (8600135) and the German–Israel Foundation for Scientific Research and Development.

* Author to whom correspondence should be addressed at the Department of Oncology, Hadassah Hospital, P.O. Box 12000, Jerusalem 91120, Israel.
‡ Department of Oncology, Hadassah University Hospital.
§ Kabi Pharmacia.
‖ Department of Medicine B, Hadassah University Hospital.

[1] Abbreviations: ECM, extracellular matrix; bFGF, basic fibroblast growth factor; HS, heparan sulfate; EC, endothelial cells; DMEM, Dulbecco's modified Eagle's medium; anti-FXa, anti-factor Xa.

0006-2960/92/0431-2080$03.00/0